Journal of Physics and Chemistry of Solids 70 (2009) 789–795

Contents lists available at ScienceDirect

Journal of Physics and Chemistry of Solids

journal homepage: www.elsevier.com/locate/jpcs

First-principles study of the optical properties of BeO in its ambient and high-pressure phases

David Groh [a,*], Ravindra Pandey [a,*], Munima B. Sahariah [b], Emilie Amzallag [c], Isabelle Baraille [c], Michel Rérat [c]

[a] Department of Physics, Michigan Technological University, Houghton, MI 49931, USA
[b] Materials Sciences Division, Institute of Advanced Study in Science and Technology, Guwahati 781035, India
[c] Université de Pau et des Pays de l'Adour, Equipe de Chimie-Physique /Institut Pluridiciplinaire de Recherche pour l'Environnement et les Matériaux (CNRS UMR5254), BP 1155, 64013 PAU Cedex, France

ARTICLE INFO

Article history:
Received 17 July 2008
Received in revised form
14 February 2009
Accepted 25 March 2009

Keywords:
A. Optical materials
D. Electronic structure

ABSTRACT

Optical properties such as the dynamic dielectric function, reflectance, and energy-loss function of beryllium oxide (BeO) in its ambient and high-pressure phases are reported for a wide energy range of 0–50 eV. The calculations of optical properties employ *first-principles* methods based on all-electron density functional theory together with sum over states and finite-field methods. Our results show subtle differences in the calculated optical properties of the wurtzite, zincblende, rocksalt and CsCl phases of BeO, which may be attributed to the higher symmetry and packing density of these phases. For the wurtzite phase, the calculated band gap of 10.4 eV corresponds well with the experimental value of 10.6 eV and the calculated (average) index of refraction of 1.70 shows excellent agreement with the experimental value of 1.72.

1. Introduction

Beryllium oxide (BeO) is a well-known prototype refractory oxide system with a wide range of applications ranging from optoelectronic devices [1] to nuclear reactors [2]. BeO occurs in the wurtzite phase at ambient conditions, although it can be transformed into high-pressure polymorphs. Its high-pressure phase transition has been studied extensively in recent decades, both theoretically and experimentally. For example, theoretical studies have previously predicted the phase transition sequence to be wurtzite to zincblende to rocksalt [3–5]. Later, it was argued [6] that an enthalpy barrier prevents the phase transition to the zincblende structure, corroborating the experimental observation [7,8] of the phase transition directly from wurtzite to rocksalt.

Since BeO is a wide-band-gap oxide crystal, its application as an ultraviolet (UV) transparent conduction oxide in flat-panel displays and solar cells can be promising. Such applications, in turn, require an accurate determination of the optical properties of BeO in its ambient phase and metastable high-pressure polymorphs in the UV region of the spectrum. Experimentally, no attempt has so far been made to perform a comprehensive study of the optical properties of BeO, though the index of refraction was measured on single crystals of synthetic bromellite [9]. Also, the polarized infrared reflection spectra in the range 400–4000 cm^{-1} were measured to study the optical phonons of BeO [10].

Recently, a theoretical study [11] has reported the real and imaginary parts of the dielectric function and energy-loss spectra of BeO in its ambient and high-pressure phases. The calculated results were based on the general-gradient approximation (GGA) within the full-potential linearized-augmented-plane-wave (FP-LAPW) method [12]. Interestingly, the FP-LAPW calculations have not reported the calculated value of the index of refraction for BeO. Furthermore, the threshold peak in the spectra of the imaginary part of the dielectric function of BeO was calculated to be at about 8.6 eV, though the band gap was measured to be 10.6 eV [13].

2. Computational method

In this letter, we employ a highly accurate method of calculating the static optical properties to study BeO in its ambient and high-pressure phases. First, we have determined the equilibrium structural properties and the associated electronic band structures using the CRYSTAL06 program package [14]. This program is based on all-electron density functional theory (DFT) in the framework of the periodic linear combination of atomic

* Corresponding authors. Permanent address: Gannon University, Erie, PA 16505, USA.
E-mail addresses: groh001@gannon.edu (D. Groh), pandey@mtu.edu (R. Pandey).

0022-3697/$ - see front matter © 2009 Elsevier Ltd. All rights reserved.
doi:10.1016/j.jpcs.2009.03.013

orbitals (LCAO) approximation. After determining the equilibrium structural and electronic properties, the static optical properties were calculated using the finite-field (FF) method [15]. The dynamic optical properties were obtained using a "sum over states" (SOS) method [16]. This method has been applied successfully to determine accurately the index of refraction, real and imaginary parts of dielectric function and energy-loss spectra of wide-band-gap systems, such as Ga_2O_3 [17], BN, GaN and MgO [18]. No attempt was made to calculate the equation of state for the ground and metastable phases of BeO since it was the focus of previous theoretical studies [3–8]. Instead we focus on calculation of the optical properties of the equilibrium configurations of the ground and metastable phases of BeO.

In the LCAO-DFT method, the exchange and correlation effects in DFT were treated by the B3LYP functional form (i.e. Becke's three-parameter hybrid exchange functional [19] and Lee, Yang and Parr correlation functional [20]). It is to be noted here that DFT calculations employing the B3LYP functional form have been found to yield band gaps for a wide variety of materials that are in good agreement with the corresponding experimental values [21,22]. A linear combination of Gaussian orbitals was used to construct a localized atomic basis from which Bloch functions are constructed by a further linear combination with phase factors. All-electron basis sets were adopted in the present study with five s- and two p-type shells for Be (i.e. a 511/11 set) [3] and eight s-, three p- and one d-type shells for O (i.e. a 8411/411/1 set) [23]. The Brillouin zone is sampled using a $12\times12\times12$ Monkhorst net for integration in the reciprocal space. We set the total energy tolerance to 10^{-7} Hartree and eigenvalue tolerance to 10^{-6} Hartree in the iterative solution of the Kohn–Sham equations.

The calculations of the static optical properties were performed with a relatively more accurate "coupled" method, which introduces a finite-field [15] perturbation in the self-consistent field (SCF) cycle as a "sawtooth" electric potential to keep the periodicity of the system [14,24]. This coupled FF method takes into account of the so-called local field effects [15,25].

As in our previous work on Ga_2O_3, a SOS method is used to calculate the real and imaginary parts of the mean dynamic polarizability $\alpha(\omega)$ of BeO as a function of the electric field frequency ω and can be written as

$$\alpha=\sum_{\vec{k}}\omega_{\vec{k}}\sum_{i,j}f_{ij\vec{k}}\left(\frac{\Delta E_{ij\vec{k}}^2-\omega^2+i\Gamma\omega}{(\Delta E_{ij\vec{k}}^2-\omega^2)^2+\omega^2\eta^2}\right) \tag{1}$$

where $f_{ij\vec{k}}$ are oscillator strengths between valence $|i>$ (occupied) and conduction $|j>$ (unoccupied) crystalline orbitals for each **k** point of the Brillouin zone with a geometric weight w_k, $E_{ij\vec{k}}$ are the corresponding vertical transition energies $\varepsilon_{j\vec{k}}-\varepsilon_{i\vec{k}}$ and η is a common value (0.3 eV) for the inverse of lifetime of the excited states. The details are given in our previous studies on Ga_2O_3 [17].

For calculations, the velocity operator $\nabla_{\vec{r}}+i\vec{k}$ used by Gajdos et al. [26] was preferred, and the transition moments between orthogonal crystalline orbitals are equal to $\langle i|\nabla_{\vec{r}}|j\rangle/(\varepsilon_{j\vec{k}}-\varepsilon_{i\vec{k}})$ instead of $\langle i|\vec{r}+i\nabla_k|j\rangle$, as the hypervirial theorem was checked [18]. We note here that, in such a gauge, the values of transition moment are very sensitive to the transition energy values between occupied and unoccupied crystalline orbitals. No scissor operator was used to correct the transition energies, but the oscillator strengths for each **k** point were multiplied by a factor such that their sum over valence occupied orbitals is equal to the number of valence electrons in the cell to obey the so-called Thomas–Reiche–Kuhn rule.

The dielectric constant can be obtained from the polarizability α of a cell as

$$\varepsilon=1+4\pi N\alpha \tag{2}$$

where N is the number of moieties per unit volume. The dynamic reflectance can now be expressed as:

$$R(\omega)=\frac{\left[1-\mathrm{Re}(\sqrt{\varepsilon(\omega)})\right]^2+\left[\mathrm{Im}(\sqrt{\varepsilon(\omega)})\right]^2}{\left[1+\mathrm{Re}(\sqrt{\varepsilon(\omega)})\right]^2+\left[\mathrm{Im}(\sqrt{\varepsilon(\omega)})\right]^2} \tag{3}$$

while the energy-loss function (ELF) is

$$\mathrm{ELF}(\omega)=\mathrm{Im}\left(-\frac{1}{\varepsilon(\omega)}\right) \tag{4}$$

3. Results and discussion

Table 1 displays the calculated structural and electronic properties of the equilibrium configurations of BeO in its ambient and high-pressure polymorphs. For the wurtzite phase, both the calculated structural and electronic properties are in excellent agreement with the corresponding experimental values. For example, the calculated lattice constant a is 2.703 Å as compared to the experimental value of 2.698 Å. [27] The calculated lattice volume is 13.80 Å^3, as compared to the experimental value [27] of 13.794 Å^3. The calculated band gap of 10.4 eV is also in excellent agreement with the experimental value [13] of 10.6 eV. Our calculations therefore show the importance of employing the B3LYP hybrid functional form and local atomic basis sets in predicting accurately the band gap of wide-band-gap oxide systems, which has been a notorious problem in DFT calculations as was the case with FP-LAPW calculations [11].

All-electron calculations allow us to calculate bands associated with the core electron levels accurately, which give important information in identifying the rearrangement of elemental electronic structure levels in a material by the photoelectron spectroscopy experiments. There is a relatively narrower O-2s located at 10.9 eV below the valence band maximum in the wurtzite phase. The O-2s band moves upward for the high-pressure NaCl and CsCl polymorphs. The calculated effective mass values of BeO are comparable to those associated with most of the

Table 1
Structural and electronic properties of the ambient and high-pressure polymorphs of BeO.

	Wurtzite	Zincblende	Rocksalt	CsCl
Crystallographic point group [31]	186	216	225	221
This work				
Energy per BeO (Hy)	−90.1481	−90.1462	−90.1064	−90.0002
Structure	$a=2.703$ Å $c/a=1.613$ $u=0.379$	3.803 Å	3.633 Å	2.331 Å
Volume per BeO (Å^3)	13.80	13.75	11.99	12.67
Be charge e	2.29	2.29	2.23	2.21
Direct gap at Γ (eV)	10.39	10.79	10.96	7.88
Effective mass m_e	0.730	0.796	0.647	0.737
O-2S band width (eV)	2.39	2.45	3.97	5.98
O-2p band width (eV)	6.58	6.53	7.83	10.1
Separation O(2s)–O(2p) (eV)	10.93	10.88	9.52	6.99
Experiment				
Structure [27]	$a=2.698$ Å $c/a=1.624$ $u=0.378$	–	–	–
Band gap [13]	10.6			
Previous theory [11]				
Structure	$a=2.639$ Å $c/a=1.629$ $u=0.377$	3.828 Å	3.651 Å	–
Direct gap at Γ (eV)	8.58	8.12	9.01	
Effective mass m_e	0.822	0.540	0.677	

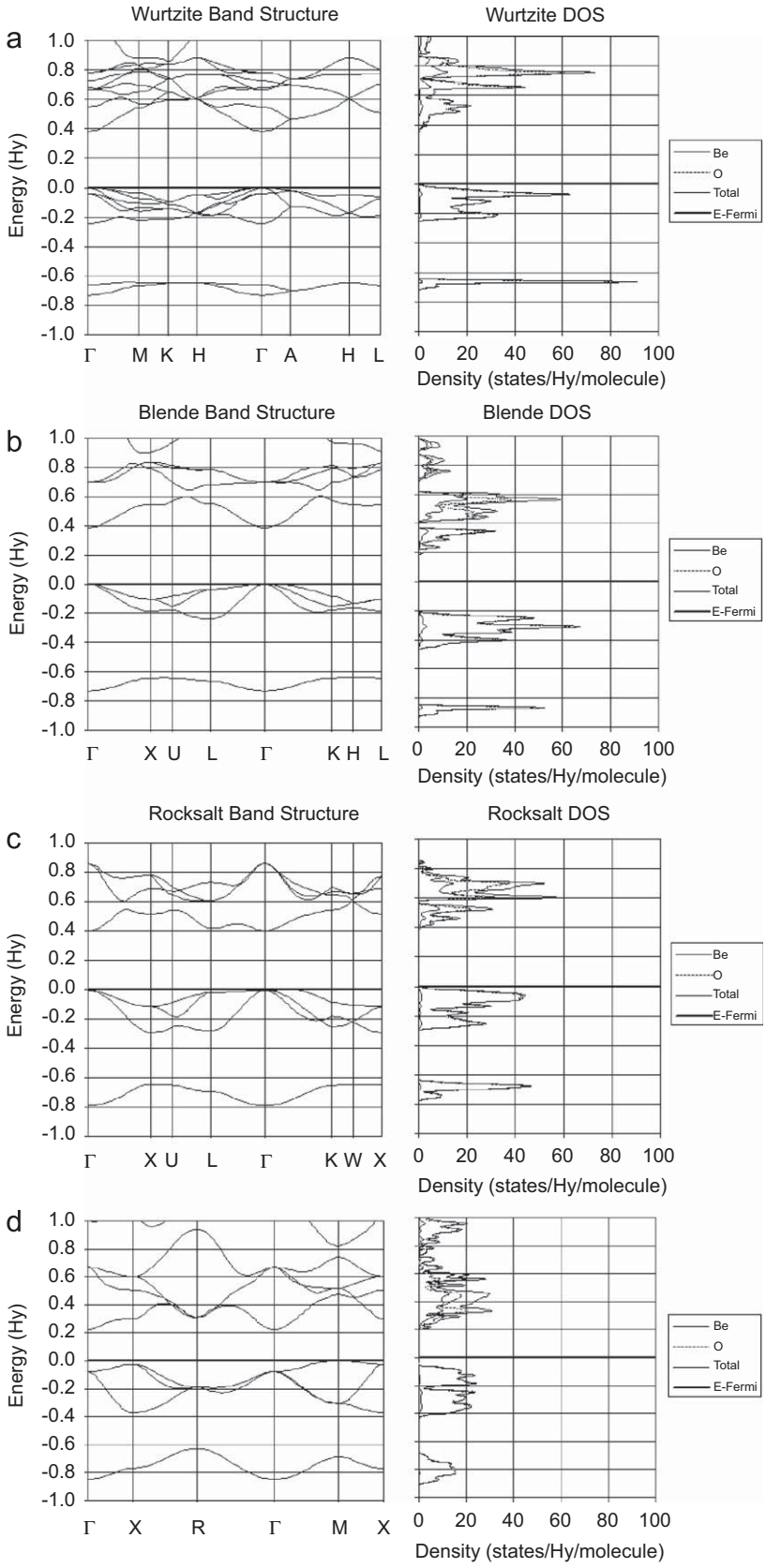

Fig. 1. Band structures and density of states for (a) wurtzite, (b) zincblende, (c) rocksalt and (d) CsCl structures of BeO.

oxide materials, suggesting that electronic conduction in BeO is possible only if electrons can be promoted to the conduction band by overcoming the large band gap.

Electronic structure calculations can predict also the nature and location of interband transitions in a crystal, which will assist the experimentalists in identifying the peaks in the optical spectra

obtained by either reflectance or photoelectron spectroscopy. Based on the electronic band structure shown in Fig. 1, absorption is predicted at 10.4, 13.3, 15.6, 16.5, 17.6, 18.1 and 19.6 eV, which are associated with interband transitions from the top of the valence band to the bottom of the conduction band at Γ, A, L, M, Γ, A and L **k** points, respectively, in the wurtzite structure of BeO. In zincblende, absorption is predicted at 10.5, 15.9, 17.6, 19.0, 19.9 and 21.5 eV, corresponding to transitions at Γ, L, X, Γ, L and X, respectively. In rocksalt, absorption is predicted at 10.8, 11.9 and 17.0 eV, corresponding to transitions at Γ, L and X, respectively. In CsCl, absorption is predicted at 8.2, 8.8, 12.9, 13.6, 14.1 and 14.5 eV, corresponding to transitions at Γ, X, M, R, M and X, respectively.

The linear response of the system to electromagnetic radiation is described by the dielectric function $\varepsilon(\omega)$ for which we consider contributions only from the interband transitions. The contributions from the intraband transitions are ignored in calculations as they are shown to be important only for metals. The real and imaginary parts of dielectric functions $\varepsilon_1(\omega)$ and $\varepsilon_2(\omega)$ are analytically and separately deduced without performing numerical integration according to the Kramers–Kronig transformation [28].

The calculated values of the optical dielectric constant ε are listed in Table 2 together with the refractive index ($n = (\varepsilon)^{\frac{1}{2}}$) for BeO in its ambient and high-pressure polymorphs; ε is obtained from the zero-frequency limit of $\varepsilon_1(\omega)$, and it corresponds to the electronic part of the static dielectric constant of the material. Since the calculated gap energy is in excellent agreement with the measured gap, the predicted dispersion of the dielectric constant will be accurate and reliable till the first resonance in the spectrum.

The dielectric constant is directly related to the polarizability of the crystal. The polarizability, which represents the deformability of the electronic distribution, is to be connected with the shape of the valence charge density. In such a highly ionic material such as BeO, oxygen ions are expected to provide the largest contribution to polarizability. In the rocksalt phase, the oxygen ions are located in an approximately cubic close-packed array, while they are located in a hexagonal close-packed array in the wurtzite phase. A similarity in dielectric as well as optical properties between these phases is expected, as was predicted in the present study. A slightly larger dielectric constant of BeO in the high-pressure CsCl phase is likely to be due to the slightly

Table 2
Dielectric constant (ε) and index of refraction (N) of BeO obtained from the finite field method.

Structure	Wurtzite	Zincblende	Rocksalt	CsCl
ε (This work)	2.90, 2.86	2.65	2.90	3.69
ε (Theory [32])	2.92			
ε (Exp. [28])	2.9730			
N (This work)	1.68, 1.72	1.63	1.70	1.92

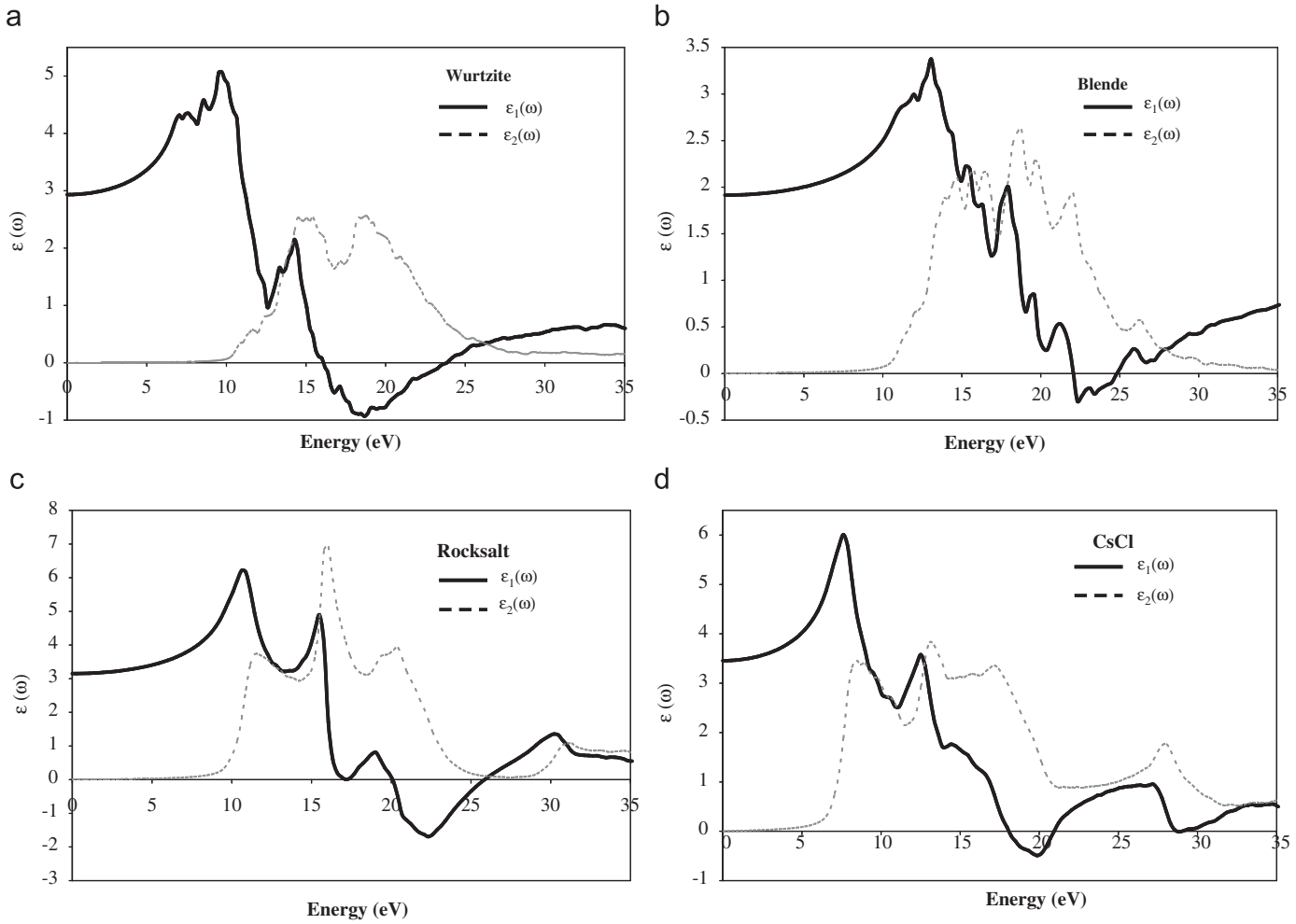

Fig. 2. Real and imaginary parts of the dielectric function for (a) wurtzite, (b) zincblende, (c) rocksalt and (d) CsCl structures of BeO.

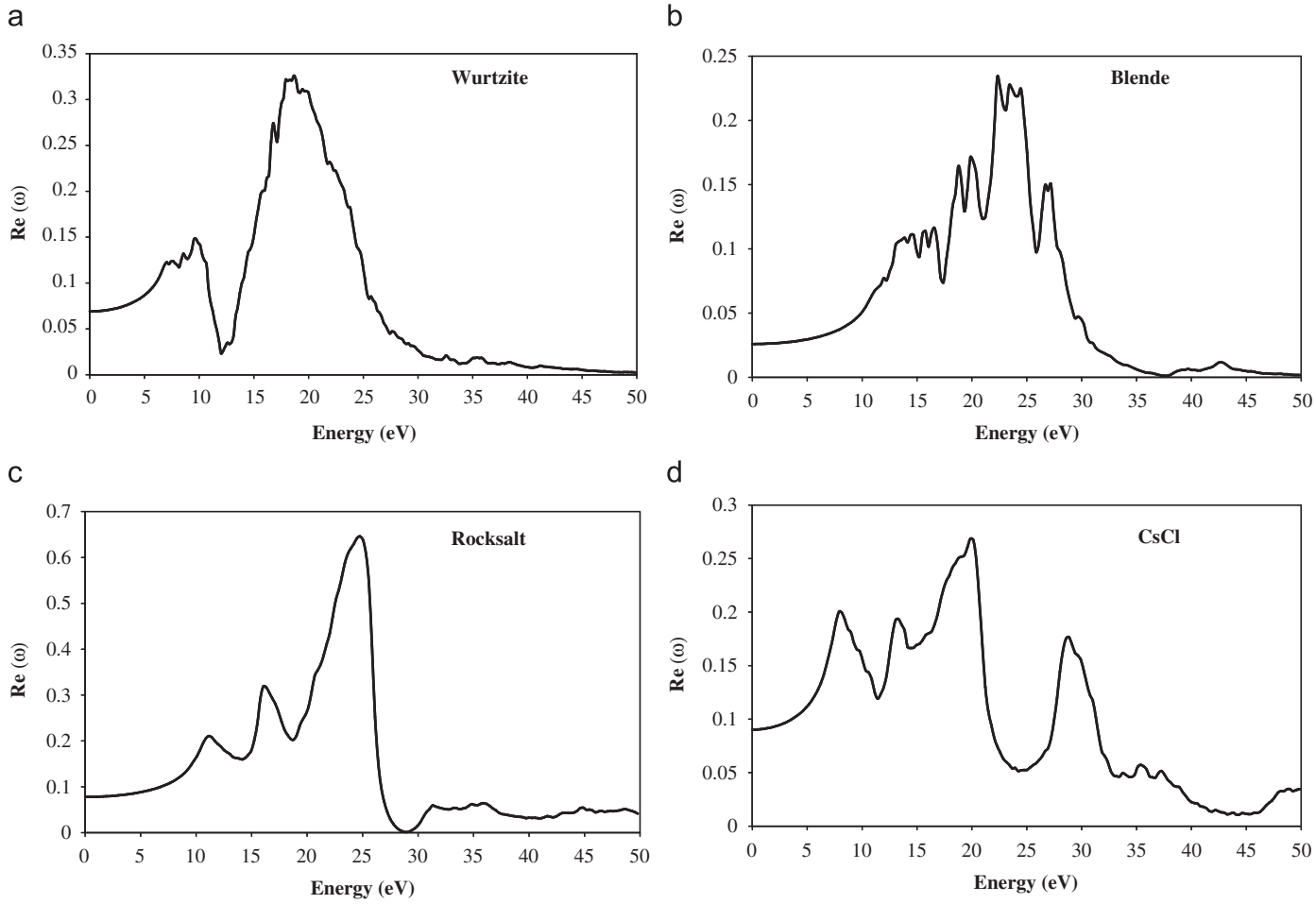

Fig. 3. Reflectivity for (a) wurtzite, (b) zincblende, (c) rocksalt and (d) CsCl structures of BeO.

denser packing of ions and higher coordination number in the lattice, which in turn reduces its band gap.

For the wurtzite phase of BeO, the dielectric property is almost isotropic with the values of the dielectric constant of 2.90 and 2.86 corresponding to the parallel and perpendicular to the *c*-axis, respectively. The respective experimental values are 2.99 and 2.95 corresponding to parallel and perpendicular to the *c*-axis [29]. The index of refraction was measured to be 1.718 and 1.733 along *a*- and *c*-axes, respectively [30]. The calculated values are 1.68 and 1.72 along *a*- and *c*-axes, respectively, showing an excellent agreement with the experimental values.

The finite-field method for determining the static (low frequency) ε yields an excellent value for comparison to experiment because it takes into account the relaxation of orbitals due to field perturbation [15]. But the FF method does not yield a frequency spectrum for $\varepsilon(\omega)$, which was calculated using the SOS method as described previously. The dispersion of the real and imaginary parts of the ε function is plotted in Fig. 2 over a wide range of energy of 0–35 eV. Their similarity is a direct reflection of similarity in the band structures of the ambient and high-pressure phases of BeO. It is an advantageous attempt of theoretical studies to identify the transitions that are responsible for the peaks in $\varepsilon_2(\omega)$ using the calculated band structures. The major peak located around 11 eV is attributed to the interband transitions from O-2p valence band to Be-2s conduction band.

The variation of reflectance as a function of photon frequency is displayed in Fig. 3. The dynamic reflectance corresponds to the ratio of the intensities of the incident and reflected electric fields. In the low-energy regime (<6 eV), the reflectance curves are nearly flat for BeO. The small value of reflectance (<0.09) in the ambient and high-pressure phases ensures application of BeO as a transparent coating in the visible–UV light regime. The spectrum shows an overall larger reflectance and a broader band in the range of 10–30 eV. This is the first time that the reflectance is presented in such a wide photon energy range of 0–50 eV. The calculated results could therefore serve as a reference for future experimental studies on BeO.

At small scattering angles, the energy-loss function is deduced from the dynamic dielectric constant using Eq. (4). The ELF spectra in Fig. 4 clearly show the energy ranges corresponding to the electronic excitations of the different orbitals. This function is important because it allows us to compare the theoretical results with spectroscopy (e.g. EELS, EXELF) measurements, which provide information about the electronic system interacting with an incident electron beam. A broad band appears in the energy range of 5–35 eV.

A significant feature in the low-loss spectrum (<50 eV) is the bulk plasmon peak, which has an intensity several orders of magnitude higher than the core-loss edges due to collective oscillation of the loosely bound electrons, which runs as a longitudinal wave through the volume of the crystal with a characteristic frequency. The plasmon energy obtained from the highest peak position are 25.4, 27.2, 23.4 and 31.7 eV for the wurtzite, zincblende, rocksalt and CsCl phases of BeO, respectively.

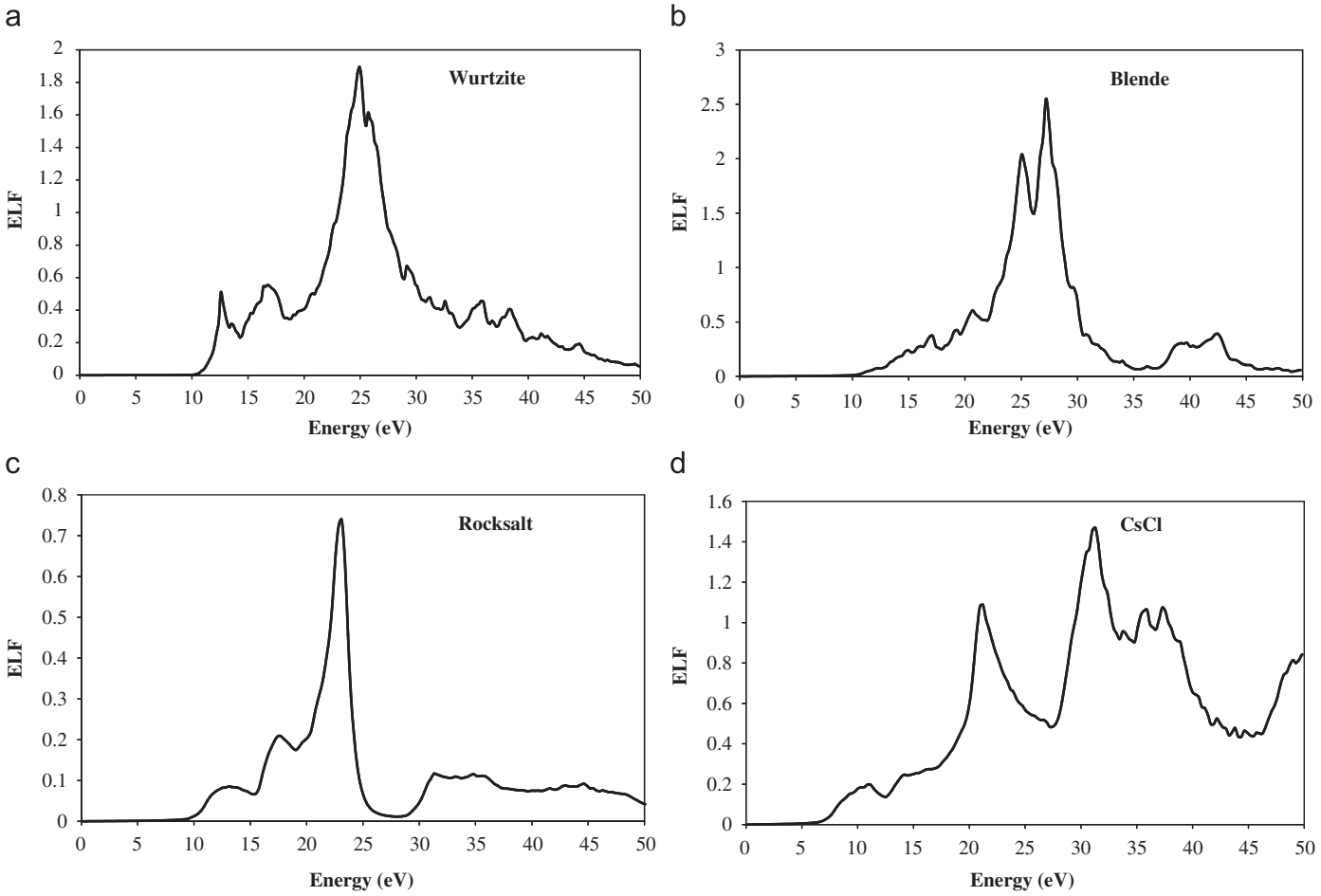

Fig. 4. Energy-loss function for (a) wurtzite, (b) zincblende, (c) rocksalt and (d) CsCl structures of BeO.

4. Summary

We have used all-electron method based on DFT to investigate the structural, electronic and optical properties of BeO in the ambient and high-pressure polymorphs. In the ambient wurtzite phase, the calculated optical properties are in an excellent agreement with the experimental values, suggesting accuracy and reliability of the method employed. The high-pressure polymorphs of BeO are predicted to show nearly the same optical properties as calculated for the wurtzite phase, though small differences can be attributed to the value of the band gap associated with the ambient or high-pressure polymorphs of BeO. For example, a higher value of dielectric constant of CsCl phase of BeO appears to be related to its relatively smaller band gap.

References

[1] V. Ivanov, M. Kirm, V. Pustovarov, A. Kruzhalov, Intrinsic luminescence in oriented BeO crystals under VUV and inner-shell excitation, Radiat. Meas. 42 (2007) 742–745.
[2] P.I.F. Zhezherun, I.P. Sadikov, V.A. Taraban'ko, A.A. Chernyshov, Measuring the moderation length of fission neutrons in sintered beryllium oxide at energies of 1.44 and 0.3 eV, At. Energy 13 (1963) 860–866.
[3] A. Lichanot, M. Chaillet, C. Larrieu, R. Dovesi, C. Pisani, Ab initio Hartree–Fock study of solid beryllium oxide: structure and electronic properties, Chem. Phys. 164 (1992) 383–394.
[4] P.E. Van Camp, V.E. Van Doren, Ground-state properties and structural phase transformation of beryllium oxide, J. Phys.: Condens. Matter 8 (1996) 3385–3390.
[5] C.J. Park, S.G. Lee, K.J. Chang, Theoretical study of the structural phase transformation of BeO under pressure, Phys. Rev. B 59 (1999) 13501–13504.
[6] Y. Cai, S. Wu, R. Xu, J. Yu, Pressure-induced phase transition and its atomistic mechanism in BeO: a theoretical calculation, Phys. Rev. B 73 (2006) 184104–184107.
[7] Y. Xu, W.Y. Ching, Electronic, optical, and structural properties of some wurtzite crystals, Phys. Rev. B 48 (1993) 4335–4351.
[8] A.P. Jephcoat, R.J. Hemley, H.K. Mao, R.E. Cohen, M.J. Mehl, Raman spectroscopy and theoretical modeling of BeO at high pressure, Phys. Rev. B 37 (1998) 4727–4734.
[9] H.W. Nowkirk, D.K. Smith, J.S. Kahn, Am. Mineral. 51 (1966) 141.
[10] E. Loh, Optical phonons in BeO crystals, Phys. Rev. 166 (1968) 673–678.
[11] B. Amrani, F.E.H. Hassan, H. Akbrazadeh, First-principles investigations of the ground-state and excited-state properties of BeO polymorphs, J. Phys.: Condens. Matter 19 (2007) 436216–436217.
[12] P. Blaha, K. Schwarz, G.K.H. Madsen, D. Kvasnicka, J. Luitz, WIEN2K—an augmented plane wave+local orbitals program for calculating crystal properties—improved and updated unix version of the original copyrighted wien-code, which was published by P. Blaha, K. Schwarz, P. Sorantin, S.B. Trickey, Full-potential, linearized augmented plane wave programs for crystalline systems, Comput. Phys. Commun. 59 (1990) 399–415.
[13] M.J. Weber, Handbook of Laser Science and Technology, vol. III, CRC Press, New York, 1986.
[14] V.R. Saunders, R. Dovesi, C. Roetti, R. Orlando, C.M. Zicovich-Wilson, N.M. Harrison, K. Doll, B. Civalleri, I.J. Bush, P. D'Arco, M. Llunell, CRYSTAL06 User's Manual, University of Torino, Torino, Italy, 2006.
[15] C. Darrigan, M. Rérat, G. Mallia, R. Dovesi, Implementation of the finite field perturbation method in the CRYSTAL program for calculating the dielectric constant of periodic systems, J. Comput. Chem. 24 (2003) 1305–1312.
[16] D. Ayma, J.P. Campillo, M. Rérat, M. Causà, Ab initio calculation of dynamic polarizability and dielectric constant of carbon and silicon cubic crystals, J. Comput. Chem. 18 (1997) 1253–1263.
[17] H. Haiying, R. Orlando, M.A. Blanco, R. Pandey, E. Amzallag, I. Baraille, M. Rérat, First-principles study of the structural, electronic, and optical properties of Ga_2O_3 in its monoclinic and hexagonal phases, Phys. Rev. B 74 (2006) 195123–195130.
[18] M. Rérat, M. Ferrero, E. Amzallag, I. Baraille, R. Dovesi, Comparison of the polarizability of periodic systems computed by using the length and velocity operators, J. Phys.: Conf. Ser. 177 (2008) 012023–012030.

[19] A.D. Becke, Density-functional exchange-energy approximation with correct asymptotic behavior, Phys. Rev. A 38 (1988) 3098–3100.
[20] C. Lee, W. Yang, R.G. Parr, Development of the Colle–Salvetti correlation-energy formula into a functional of the electron density, Phys. Rev. B 37 (1998) 785–789.
[21] J. Muscat, A. Wander, N.M. Harrison, On the prediction of band gaps from hybrid functional theory, Chem. Phys. Lett. 342 (2001) 397–401.
[22] H. Jiang, R. Orlando, M.A. Blanco, R. Pandey, First-principles study of the electronic structure of PbF_2 in the cubic, orthorhombic, and hexagonal phases, J. Phys.: Condens. Matter 16 (2004) 3081–3088.
[23] T. Bredow, K. Jug, R.G. Parr, Electronic and magnetic structure of $ScMnO_3$, Phys. Status Solidi (b) 243 (2006) R10–R12.
[24] R. Resta, K. Kunc, Self-consistent theory of electronic states and dielectric response in semiconductors, Phys. Rev. B 34 (1986) 7146–7157.
[25] M. Rérat, R. Dovesi, Elongation method at semi-empirical and ab initio levels for large systems, in: Proceedings of the International Conference of Computational Methods in Sciences and Engineering, vol. 1, 2004, pp. 771–774.
[26] M. Gajdos, K. Hummer, G. Kresse, J. Furthmüller, F. Bechstedt, Linear optical properties in the projector-augmented wave methodology, Phys. Rev. B 73 (2006) 045112–045120.
[27] R.M. Hazen, L.W. Finger, High-pressure and high-temperature crystal chemistry of beryllium oxide, J. Appl. Phys. 59 (1986) 3728–3733.
[28] S.D. Mo, W.Y. Ching, Electronic and optical properties of three phases of titanium dioxide: rutile, anatase, and brookite, Phys. Rev. B 51 (1995) 13023–13032.
[29] D.R. Lide, Handbook of Chemistry and Physics, 71st ed., CRC Press, New York, 1991.
[30] Yen Tung-Sheng, et al., Phase equilibria in the systems rare-earth sesqui-oxide-beryllium oxide, J. Am. Ceram. Soc. 66 (1983) 860–862.
[31] Crystal Lattice Structures Web page, 〈http://cst-www.nrl.navy.mil/lattice/〉, provided by the Center for Computational Materials Science, United States Naval Research Laboratory.
[32] F. Kootstra, P.L. de Beoeij, J.G. Sniders, Application of time-dependent density-functional theory to the dielectric function of various nonmetallic crystals, Phys. Rev. B 62 (2000) 7071–7083.